Experimental Study of the Effects of Nonlinearities on Ground Resonance

George T. Flowers*
Auburn University, Auburn, Alabama 36849
and
Benson H. Tongue†
University of California, Berkeley, Berkeley, California 94720

An experimental investigation into the effects of nonlinearities on the ground resonance behavior of rotorcraft is conducted and the results correlated with analytical predictions. The experimental techniques and results are described in detail and representative graphs of the observed behavior are shown and discussed. It is found that responses of destructively high amplitude may occur in systems for which a linear analysis predicts stable behavior.

Nomenclature

b = number of rotor blades
c_b = linear blade damping
c_x = linear roll (x) damping
c_y = linear pitch (y) damping
$\tilde{c}_b = c_b/\omega_0$
$\tilde{c}_x = c_x/\omega_0$
$\tilde{c}_y = c_y/\omega_0$
f_b = frictional blade damping
$\tilde{f}_b = f_b/\omega_0^2$
f_{db} = total nonlinear blade damping
$\tilde{f}_{db} = f_{db}/\omega_0^2$
f_{dx} = total nonlinear roll (x) damping
$\tilde{f}_{dx} = f_x/\omega_0^2$
f_{dy} = total nonlinear pitch (y) damping
$\tilde{f}_{dy} = f_y/\omega_0^2$
f_x = frictional roll (x) damping
$\tilde{f}_x = f_x/\omega_0^2$
f_y = frictional pitch (y) damping
$\tilde{f}_y = f_y/\omega_0^2$
g_b = hydraulic blade damping
$\tilde{g}_b = g_b$
g_x = hydraulic roll (x) damping
$\tilde{g}_x = g_x$
g_y = hydraulic pitch (y) damping
$\tilde{g}_y = g_y$
h = height of rotor above gimbal support
h_b = cubic blade damping
$\tilde{h}_b = \omega_0 h_b$
h_x = cubic roll (x) damping
$\tilde{h}_x = \omega_0 h_x$
h_y = cubic pitch (y) damping
$\tilde{h}_y = \omega_0 h_y$
I_b = blade mass moment of inertia
I_x = inertia about roll (x) axis
I_y = inertia about pitch (y) axis
L = blade length
l_{vh} = blade lagging hinge offset
p_b^2 = linear blade stiffness
p_x^2 = linear roll (x) stiffness
p_y^2 = linear pitch (y) stiffness
$\tilde{p}_b^2 = p_b^2/\omega_0^2$
$\tilde{p}_x^2 = p_x^2/\omega_0^2$
$\tilde{p}_y^2 = p_y^2/\omega_0^2$
S = first moment of blade inertia about the lag hinge
ω = rotor speed
ω_0 = nominal rotor speed
$\tilde{\omega}$ = nondimensional rotor speed ω/ω_0
$\psi_k = \omega t + (k\pi/b)$

Subscript

k = blade index number

Superscripts

$\cdot$ = derivative with respect to time
$'$ = derivative with respect to τ

Introduction

ALTHOUGH the techniques for studying linear systems are very well developed, the modeling and analysis of nonlinear systems is, at best, a difficult undertaking and, for large order systems, a nearly impossible task. For these reasons, most modeling and analysis that is performed on dynamical systems is done under the assumption that the behavior of interest can be accurately described by a linear model. For many mechanical systems, such linear models provide a good approximation to the actual system. However for systems with strong nonlinearities, linear models yield results that poorly approximate the observed behavior. Helicopters are highly nonlinear devices and it is thus of interest to determine how various nonlinearities affect their behavior. In this study, a particular mode of helicopter vibration known as ground resonance is examined for the effect of nonlinearities on the observed responses.

The ground resonance phenomenon is a highly destructive instability that can occur when a helicopter is in contact with the ground. It has been observed since the early days of helicopter development, and a number of helicopters have been destroyed or badly damaged as a result of its effects. Work by Coleman and Feingold,[1] using a linear model, indicates that linearly unstable responses can occur over a finite range of

Received June 3, 1988; revision received March 20, 1989.

*Assistant Professor, Mechanical Engineering.
†Associate Professor, Mechanical Engineering.

rotor speeds, as shown in Fig. 1. This research indicates that increasing the system damping tended to decrease the extent of the rotor speed regime that leads to unstable behavior. Ground resonance has been countered using a number of different approaches suggested by linear analyses, including the inclusion of dampers for the lead-lag motions of the rotor set and designing of the nominal helicopter operating speed so as to avoid the rotor-speed range in which destructive vibrations can develop.

A question can be raised as to how nonlinear effects can alter the behavior one might expect from the results of a linear analysis. Intuitively, one might expect finite amplitude limit cycles to exist within the linearly unstable region if nonlinear restoring forces were sufficient to counter the linearly destabilizing effects. Although such behavior does occur, work by Tongue[2] indicates that it was possible to have responses of destructively high amplitude at rotor speeds that are outside of the linearly unstable regime (see Fig. 2). These results were obtained from an examination of a single-degree-of-freedom fuselage with hydraulic damping nonlinearities in the landing gear. This work was later extended to consider damping nonlinearities in the blades.[3] Tang and Dowell[4] added a degree of freedom to the fuselage model and used Tongue's iterative solution technique to locate limit cycles for the case of nonlinearities in the blades and landing gear. In this work the nonlinearities also included a dry frictional damping term. The analytical solutions did not consider the full effect of geometric nonlinear terms but was restricted to a retention of second-order terms. Some experimental results that were in reasonable agreement with the theoretical predictions were given. One finding was that for a large initial disturbance, the actual model exhibited an oscillatory growth, rather than the decay predicted by the theory, an effect that was attributed to problems in the parameter identification. Finally, in Ref. 5, Tang and Dowell presented the equations of motion for a model in which both the rotor and the fuselage possessed pitch and roll degrees of freedom. Three simplified cases were examined and compared to experimental results. Again, the nonlinear terms were dry friction and hydraulic nonlinearities. In addition to finding a reasonable match between theory and experiment, they noted that small differences in the properties of the individual blade damping led to differences in the individual blade limit cycle behavior.

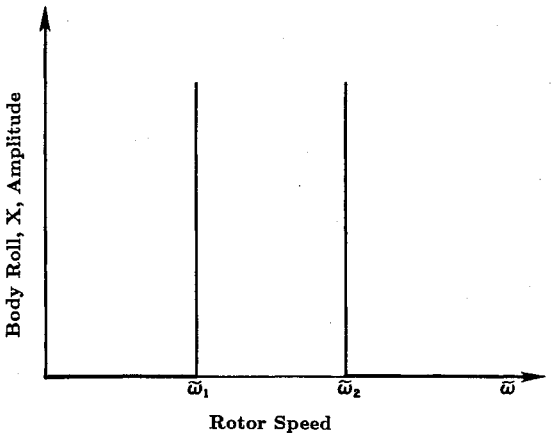

Fig. 1 Amplitude of body motion vs rotor speed for the linear ground resonance model.

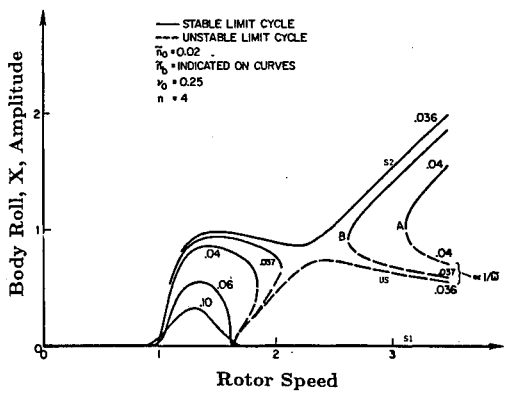

Fig. 2 Amplitude of body motion vs rotor speed for the ground resonance model with a nonlinear landing gear damper.

In the present study, experimental responses and analytical predictions are correlated. The experimental model, although linearly stable for all rotor speeds under a linear analysis, is shown to exhibit finite amplitude limit cycle responses. Thus, it is shown that a linearized analysis for studying the ground resonance behavior of a rotorcraft does not give a conservative estimate of the craft's responses, and the use of such linearized models in design or analysis work could lead to difficulties. Essentially, the results suggest that a linearly stable craft, subjected to a hard excitation (such as a hard landing), can exhibit a destructive response.

Analytical Model

Assumptions

The experimental model consists of a rotor attached to a gimballed support, which is restrained by springs and dampers (see Fig. 3). The allowable motions consist of rotations about two axes.

To develop a suitable ground resonance model, the following assumptions were made:

1) The body was modeled as a rigid body.
2) Body motion was limited to roll and pitch about the body center of mass.
3) Gravitational effects were neglected.
4) Rotor dynamics were modeled using four identical, equally spaced, rigid blades with root springs and dampers.
5) Rotor speed was constant.
6) Inertia of blades about the blade pitch axis was neglected.
7) Tail rotor dynamics were neglected.
8) Aerodynamical effects were neglected.

Whereas these assumptions produce a greatly simplified model, the full nonlinear equations of motion are still quite lengthy and contain many terms.[6] Further simplifications must be made if the equations are to be analyzed. The procedure used in this study consisted of examining the relative contribu-

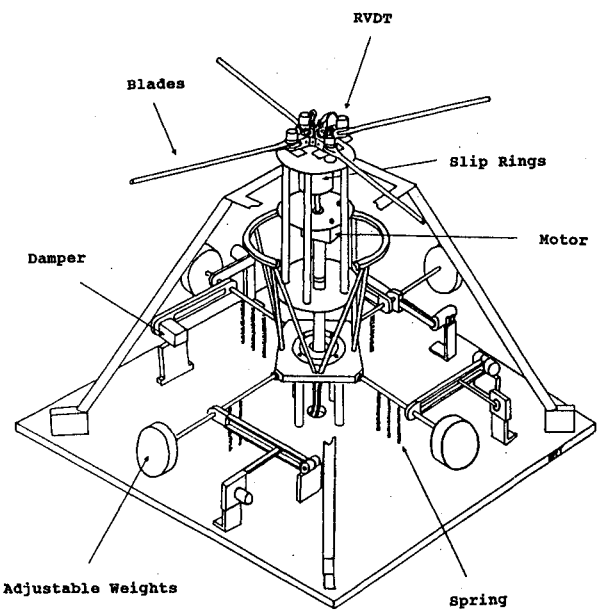

Fig. 3 Experimental ground resonance model.

tion of each of the nonlinear terms to the overall response. This study indicates that, for the cases examined, the nonlinear damping terms were the primary nonlinear effect. The effects of the other nonlinear terms were negligible in comparison. The model was reduced by linearizing about an equilibrium operating condition and adding selected nonlinearities in the form of damping terms.

The simplified dynamical equations that resulted were

$$I_x\ddot{x}+F_{dx}+p_x^2x=hS\sum_{k=1}^{N}\left[\ddot{\xi}_k\sin(\psi_k)+\omega^2\xi_k\cos(\psi_k)-2\omega\dot{\xi}_k\sin(\psi_k)\right] \quad (1)$$

$$I_y\ddot{y}+F_{dy}+p_y^2y=-hS\sum_{k=1}^{N}\left[\ddot{\xi}_k\cos(\psi_k)-\omega^2\xi_k\sin(\psi_k)-2\omega\dot{\xi}_k\cos(\psi_k)\right] \quad (2)$$

$$I_b\ddot{\xi}_k+F_\xi+p_b^2\xi_k+l_{vh}S\omega^2\xi_k=hS\left[\ddot{x}\sin(\psi_k)-\ddot{y}\cos(\psi_k)\right] \quad (3)$$

The parameter variation studies performed in this research were done by altering the physical components of the model that are relatively easy to quantitize, i.e., the body inertias, blade lengths, and body stiffnesses. As a result, it is not desirable to completely nondimensionalize the equations of motion. However, it is desirable to express them in nondimensionalized time form so that the relative rotor speeds can be more easily understood. If the time scale τ is introduced, where $\tau=\omega t$, then Eqs. (1-3) become

$$I_xx''+\tilde{F}_{dx}+\tilde{p}_x^2x=hS\sum_{k=1}^{N}\left[\xi_k''\sin(\psi_k)+\tilde{\omega}^2\xi_k\cos(\psi_k)-2\tilde{\omega}\xi_k'\sin(\psi_k)\right] \quad (4)$$

$$I_yy''+\tilde{F}_{dy}+\tilde{p}_y^2y=-hS\sum_{k=1}^{N}\left[\xi_k''\cos(\psi_k)-\tilde{\omega}^2\xi_k\sin(\psi_k)-2\tilde{\omega}\xi_k'\cos(\psi_k)\right] \quad (5)$$

$$I_b\xi_k''+\tilde{F}_\xi+\tilde{p}_b^2\xi_k+l_{vh}S\tilde{\omega}^2\xi_k=hS\left[x''\sin(\psi_k)-y''\cos(\psi_k)\right] \quad (6)$$

The primary nonlinearities that are retained are those associated with the damping of the system.

Limit Cycle Analysis

In an earlier paper,[6] a detailed discussion of the limit-cycle analysis of Eqs. (4-6) is given. The essence of this approach is to represent each of the dynamical variables as a sinusoid at a given frequency. These terms are then substituted into the nonlinear equations, and Galerkin averaging is applied to retain only those oscillations that occurred at the assumed frequency. If higher harmonics are not significant in the output of the integrated equations, then neglecting these terms will not significantly impair the accuracy of the limit-cycle determination.

To carry out the fully nonlinear analysis, motion of the following form is assumed:

$$\xi_1=A\cos(\omega_bt) \quad (7)$$

$$\xi_2=-A\sin(\omega_bt) \quad (8)$$

$$\xi_3=-A\cos(\omega_bt) \quad (9)$$

$$\xi_4=A\sin(\omega_bt) \quad (10)$$

$$x=X_c\cos(\omega_gt)+X_s\sin(\omega_gt) \quad (11)$$

$$y=Y_c\cos(\omega_gt)+Y_s\sin(\omega_gt) \quad (12)$$

Note that, based on the numerical investigations, the assumption is made that ω is equal to $\omega_g+\omega_b$. The limit cycle methodology stems from the observation that Eqs. (7-12) should be good approximations to the actual response, as seen in the numerical simulations. If Eqs. (7-12) are substituted into Eqs. (4-6) and all spectral components expanded out, one would expect to generate a large variety of spectral responses, i.e., responses at ω_g, ω_b, $\omega+\omega_g$, etc. Logically, all harmonics other than those at ω_g for the body and those at ω_b for the blades should cancel out of the resulting equations. Therefore, an accurate set of equations for the limit-cycle amplitudes should be obtained by simply retaining those terms that yield responses at ω_g for Eqs. (4) and (5) and at ω_b for Eq. (6). The preceding methodology was implemented, resulting in a set of algebraic equations.

Solutions to the equations for fixed parameter values and varying rotor speeds were found using a numerical analysis procedure employing the Newton-Raphson technique.

Experimental Study

Experimental Apparatus

The basic structure of the experimental rotorcraft model was designed at Princeton University in the 1960s by Richard Bielawa. The original design was meant to serve as an approximate scale model for the Hiller light observation helicopter. It was later used at Duke University by Earl H. Dowell and D. M. Tang. This model was donated to the present project by Howard C. Curtiss, Professor of Mechanical and Aerospace Engineering at Princeton University. A schematic of the structure is shown in Fig. 3. The inertia, stiffness, and damping of the gimballed shaft are adjustable.

The original model has been substantially modified in several ways. The rotor system initially had three blades, each of which had an attached airfoil. The three-bladed rotor head was replaced with a four-bladed design to allow direct comparisons with previous work.[2] As suggested by Bousman,[8] rods with a circular cross section were used instead of conventional blades equipped with airfoils. The effect of the circular cross section is to reduce the slope of the lift curve to zero to simulate in vacuo conditions. This can be seen in the following way. The Lock number is a measure of the effect of aerodynamic forces on the blade dynamics and is defined as

$$\Gamma=\rho cL^4/I_b(a+C_{d0})$$

For a zero lift slope, the magnitude of the Lock number is reduced to about 0.2% of the value it would be if conventional aerodynamic blades were used.[7]

The speed of the motor installed originally on the model was controlled by varying the resistance in the power supply lines and so changing the amount of current supplied. Preliminary testing indicated that this method of speed control permitted speed variation of several radians per second, particularly as the temperature of the resistance coil began to increase. One of the primary assumptions of the previous analyses has been the constancy of the rotor speed. Thus, a more precise control was required. A motor equipped with a feedback torque and speed controller was installed on the craft. Testing of this unit showed that the rotor speed varied less than 0.2 rad/s and was judged to provide acceptable speed control.

Measurement Apparatus

Rotary variable differential transformers (RVDT) were used to measure the angular motion of the fuselage and blades. Voltage amplifiers provided ± 15 V dc to the RVDTs and a reference signal for a mechanical switching assembly used to measure the rotor speed. Capture of the analog signals from the RVDTs was accomplished with an RTI-800 multifunction

input/output board. Eight channels for differential inputs were available on this board. Six of the channels were used to obtain readings of the blade and rotor positions, and one channel served as an input for the signal from the speed measurement apparatus. The board was configured to read input signals of ±10.0 V, which were converted by a 12-bit, analog-to-digital converter with a resolution of 12 bits and stored in the memory of an IBM PC/XT, which served as the controller for this data acquisition system. The data acquisition software was written in BASIC and compiled. A complete reading of all seven of the input channels could be performed approximately every 0.03 s, which was quite sufficient for the low-frequency signals encountered in this study. Tests of this system showed that the measured signals had only low levels of contaminating noise, and it was therefore felt that additional filtering was unnecessary.

Parameter Identification

In any experimental investigation, it is of critical importance to be able to determine the parameters of the experimental apparatus. This is particularly true in this case, as the correct determination of the system parameters, both linear and nonlinear, is crucial to any conclusions that are to be drawn. The parameters were estimated by several different procedures and, where possible, the resulting parameters were cross checked using alternate methods.

The parameters S, I_b, I_x, and I_y were calculated directly from a knowledge of the individual mass and length of the structural elements. The fuselage stiffnesses were calculated from tests of the natural frequency of oscillation with the dampers removed and the blades locked and from direct measurement of the displacement caused by a specified force.

As is true with most mechanical systems, the damping of the experimental model was difficult to characterize. The inclusion of different types of damping in the analytical test procedure indicated that frictional, linear, hydraulic, and cubic terms were required to provide an accurate model of the system damping. So, polynomial damping functions of the following form were assumed for the blade and body damping.

$$\tilde{F}_x = \tilde{c}_x x' + \tilde{h}_x x' |x'| + \tilde{g}_x x'^3 + \tilde{f}_x \operatorname{sign}(x')$$

$$\tilde{F}_y = \tilde{c}_y y' + \tilde{h}_y y' |y'| + \tilde{g}_y y'^3 + \tilde{f}_y \operatorname{sign}(y')$$

$$\tilde{F}_\xi = \tilde{c}_\xi \xi'_k + \tilde{h}_\xi \xi'_k |\xi'_k| + \tilde{g}_\xi \xi'^3_k + \tilde{f}_\xi \operatorname{sign}(\xi'_k)$$

The experimental procedure for determining the fuselage damping consisted of attaching a mass to the end of one blade and locking the blades to the rotor hub so that lead-lag motion was eliminated. This resulted in a sinusoidal excitation of the fuselage when the rotor was allowed to rotate. A proximity sensor was used to trigger the data acquisition system so that the phase between the motion of the rotor head and the motion of the fuselage could be determined. Responses for several different rotor speeds were measured, and the body damping and stiffnesses were estimated using a least-squares fit of the data from each of the speeds. This is in effect averaging the parameters over several different sets of data. The results were quite good in general. For four or more sets of the data, the identification routine converged well with good consistency and realistic parameters.

Determination of the blade damping was more difficult. Two techniques were used that gave comparable results. The first consisted of recording the impulse response of each of the blades and fitting a polynomial curve to the resulting data. The equation for the trajectory could then be differentiated with respect to time and substituted into the equation of motion for the rotor blade. Then, a least-squares identification routine was used to identify the blade-damping parameters assuming the presence of frictional, linear, hydraulic, and cubic damping. The second approach consisted of minimizing an error function based on the weighted differences between the experimentally determined amplitudes and frequencies and the analytically determined ones for limit-cycle motion of the model. The analytical values are found from the solutions of the nonlinear set of algebraic equations produced by a harmonic balance of the equations of motion. In the identification, it is vital that a first estimate for the parameters be close to actual parameter values so that convergence will occur. For the cases studied here, the parameters from the impulse response were used for the initial parameter values. Typical blade and body parameters are shown in Table 1.

Test Procedure

The test procedure has consisted of varying the rotor speed and perturbing the system with an input to the fuselage until a steady oscillation of the model on its gimballed support is observed. Then, after the oscillations appear to have stabilized, readings of the position for each of the fuselage and blade motions were recorded for approximately 1 min. This data was transferred from the IBM PC/XT to a VAX 11/750 and processed to transform the voltage readings of the RVDTs to angular position in radians. The resulting information was then Fourier analyzed to determine the frequencies and amplitudes of the responses.

Experimental Results

A series of parameter variation studies was performed on the experimental model. It is important to notice that the

Table 1 Typical experimental model parameters

Parameter	Value	Units
S	0.0202	lb-s^2
h	21.0	in.
l_{vh}	3.0	in.
I_b	0.3347	lb-in.-s^2
I_x	17.8	lb-in.-s^2
I_y	12.9	lb-in.-s^2
$\tilde{c}_b$	0.0518	lb-in.-s^2
$\tilde{c}_x$	2.37	lb-in.-s^2
$\tilde{c}_y$	2.37	lb-in.-s^2
$\tilde{g}_b$	−0.0669	lb-in.-s^2
$\tilde{g}_x$	−66.5	lb-in.-s^2
$\tilde{g}_y$	−66.5	lb-in.-s^2
$\tilde{f}_b$	0.0005	lb-in.-s^2
$\tilde{f}_x$	0.0001	lb-in.-s^2
$\tilde{f}_y$	0.0001	lb-in.-s^2
$\tilde{h}_b$	5.19	lb-in.-s^2
$\tilde{h}_x$	1176.3	lb-in.-s^2
$\tilde{h}_y$	01176.3	lb-in.-s^2
$\tilde{k}_x$	5.827	in.-lb-s^2
$\tilde{k}_y$	4.57	in.-lb-s^2
ω_0	15.5	rad/s

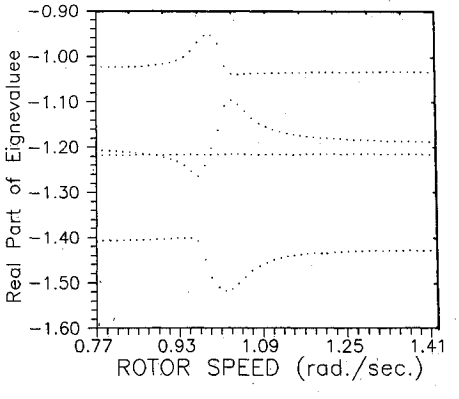

Fig. 4 Eigenanalysis for ground resonance model.

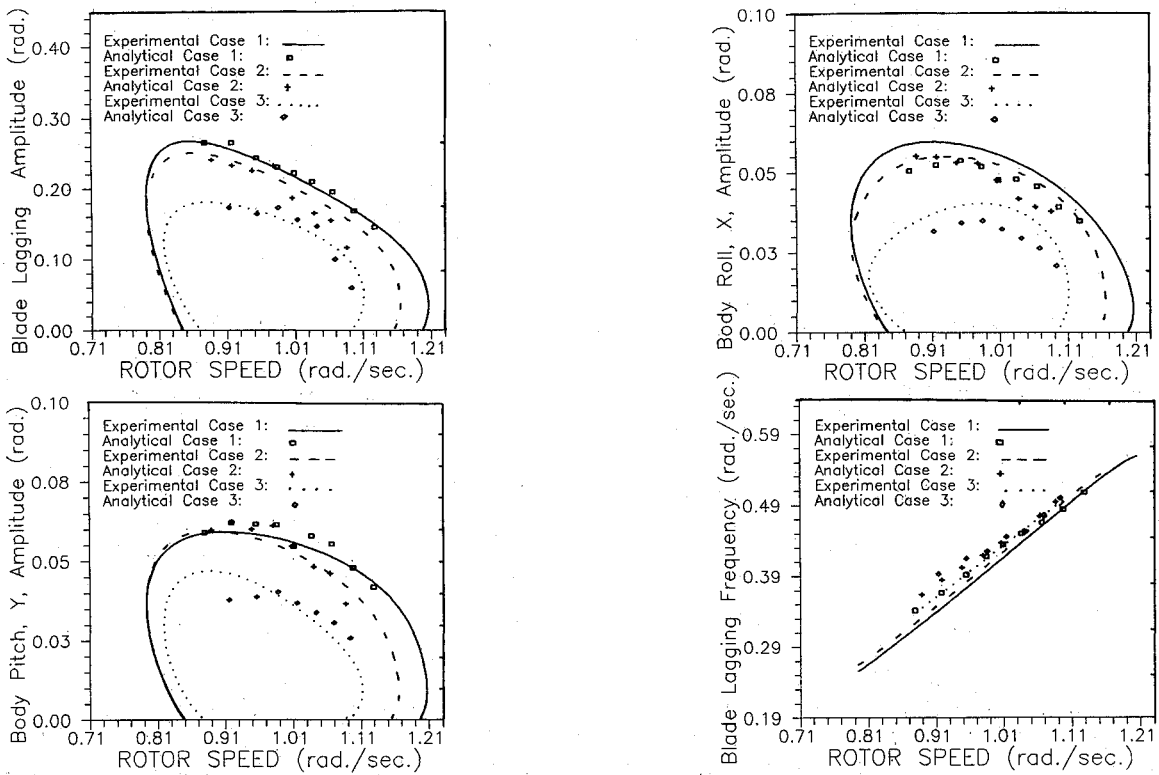

Fig. 5 Experimental responses for varying body inertias: case 1, $I_y = 12.9$ in.-lb-s^2; case 2, $I_y = 14.25$ in.-lb-s^2; and case 3, $I_y = 16.0$ in.-lb-s^2.

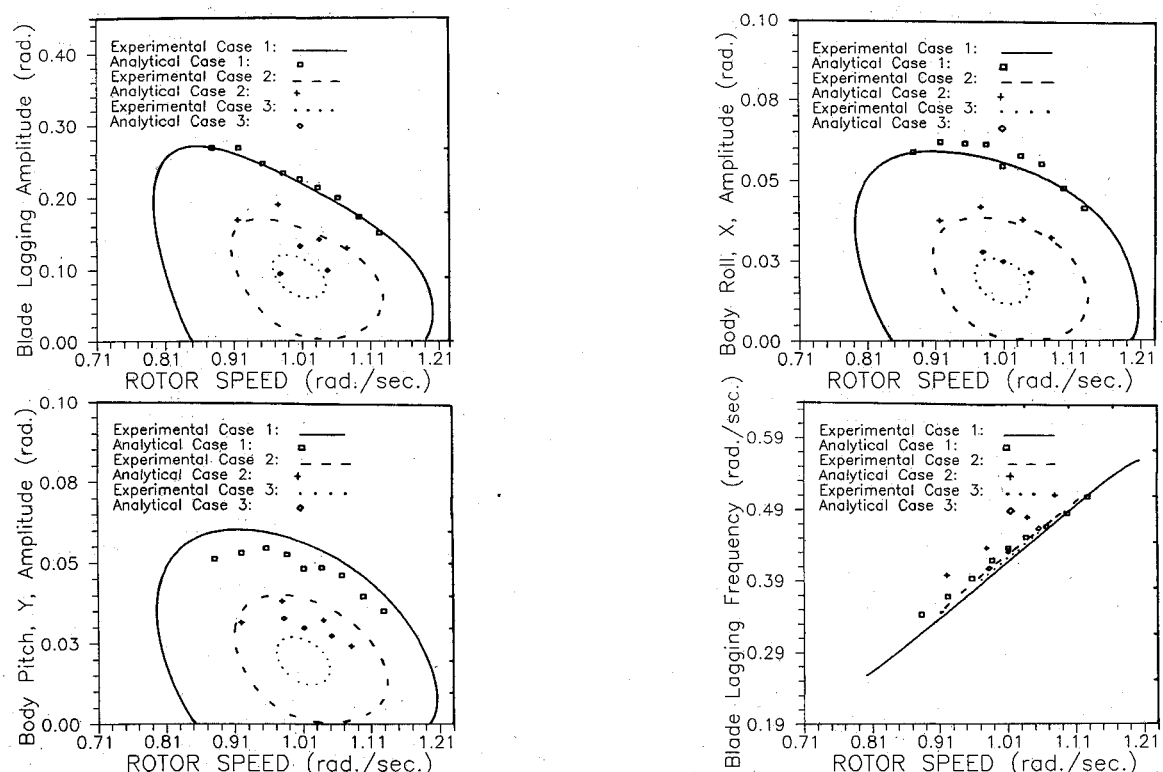

Fig. 6 Experimental responses for varying blade lengths: case 1, $L = 20.5$ in., $I_b = 0.335$ lb-in.-s^2, $S = 0.020$ lb-s^2; case 2, $L = 17.5$ in., $I_b = 0.270$ lb-in.-s^2, $S = 0.018$ lb-s^2; and case 3, $L = 16.5$ in., $I_b = 0.260$ lb-in.-s^2, $S = 0.017$ lb-s^2.

observed responses are for a model that is linearly stable. That is, an analysis of the linear system would show that the steady state responses are of zero amplitude and the response to an initial perturbation will decay to zero, as indicated by the fact that all eigenvalues have negative real parts (Fig. 4). Nonzero responses are seen because the system is perturbed beyond the region of linear stability so that nonlinear effects become important. As a result, finite amplitude limit cycles are observed. Figures 5–7 show experimental results and the corresponding analytical correlations. For each of these studies, the parameters for case 1 are shown in Table 1. The parameters for case 2 and case 3 are the same as for case 1 except as indicated on each of the plots.

Experimental measurements were performed for a variety of parameter configurations and a wide range of rotor speeds. Tests were conducted in which one particular parameter was varied and the responses measured and analyzed at various rotor speeds for each parameter value. Studies were performed in which the fuselage stiffnesses, blade lengths, and fuselage inertias were varied.

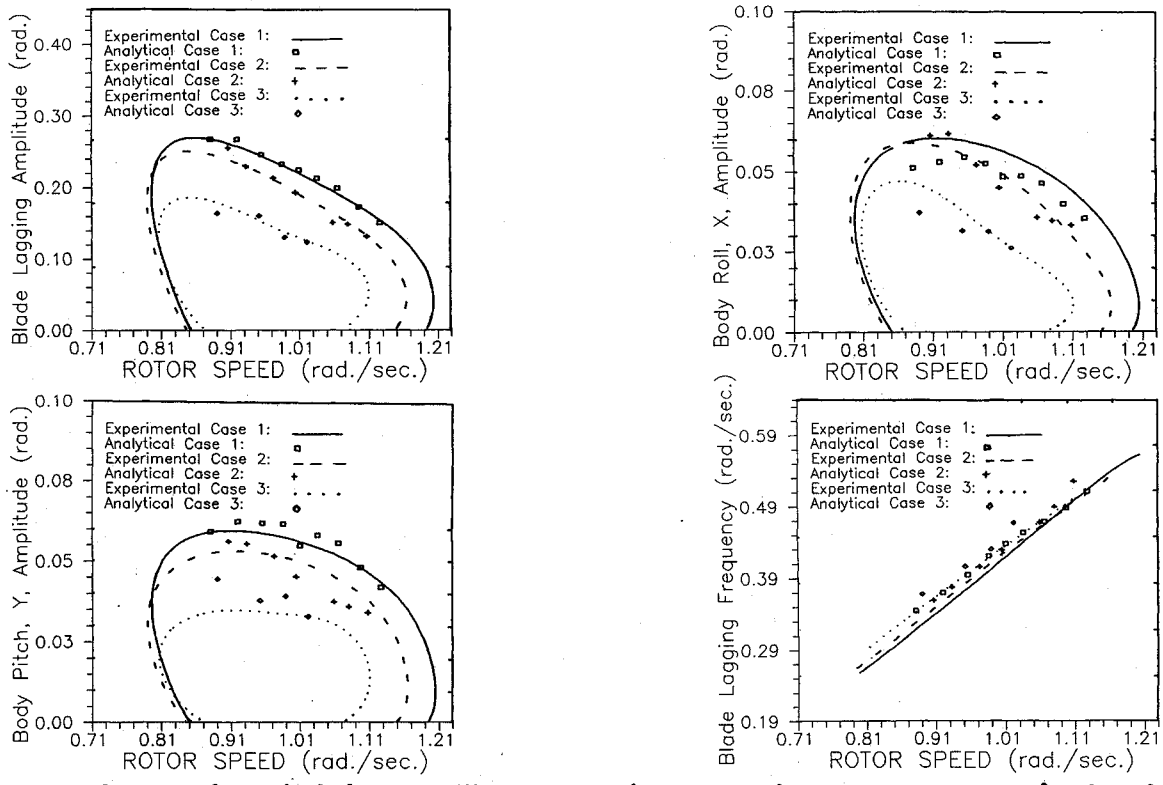

Fig. 7 Experimental responses for varying body support siffnesses: case 1, $p_{\dot{y}_2}^2 = 6.05$ in.-lb-s^2; case 2, $p_{y_2} = 5.57$ in.-lb-s^{-2}; and case 3, $p_y = 5.02$ in.-lb-s^{-2}.

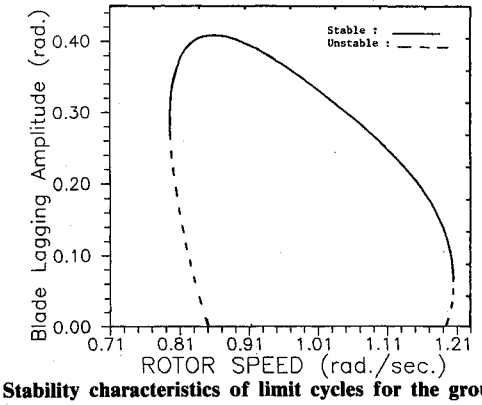

Fig. 8 Stability characteristics of limit cycles for the ground resonance model.

The responses obtained as the y fuselage inertia was varied are shown in Fig. 5. The amplitudes of the blade-lag and fuselage motions show excellent correlation with the analytically predicted responses for a rotor speed range of about 14.5–17.8 rad/s. The lag amplitudes decrease steadily from a peak response at 14.5 rps to the lowest measureable response at between 16.8 and 17.8 rps for the different curves. Notice that the peak responses are at approximately the same location, both experimentally and analytically. For the fuselage motion, good correlation between analytical predictions and experimental results was obtained, although the results were slightly better for the x motion. The predicted frequences were consistently lower by about 10% than the measured frequencies, but the general trend of slightly increasing frequency as the fuselage inertia is increased is captured very well.

The responses obtained as the blade length was varied are shown in Fig. 6. The analytical predictions and the measured responses correlate well. The results are quite interesting. Note the analytically predicted responses are almost concentric curves with a center at a rotor speed of about 15.8 rps and a blade-lag amplitude of 0.085 rad. The measured responses for the blade lag amplitudes differ from the predicted values by no more than 15% with most of the values corresponding almost exactly. The measured fuselage responses match the analytically predicted responses quite well. The blade-lag frequencies are consistently above the predicted values, but the difference is never more than about 10% and the trend of the experimental results is followed rather nicely.

The responses obtained for the variation of the x fuselage spring stiffness are shown in Figs. 7. The experimental and analytical results again demonstrated an excellent correlation for the blade-lag amplitudes. The experimental and analytically predicted responses for the fuselage amplitude also match very well. The blade-lag frequencies are consistently about 5% above the predicted values, but the general trend of slightly increasing frequency as the x fuselage stiffness is decreased is captured very well by the analysis results.

All of the response plots have several common features. The responses can be tracked from higher rotor speeds to lower rotor speeds with relative ease, but difficulty is encountered when one attempts to track the responses in the opposite direction. For each of the studies, the responses drop from a finite amplitude to zero amplitude abruptly rather than in the continuous manner predicted by the analysis. Such behavior was consistently observed for all tests. A study of the analytically predicted responses shows clearly why this is true. Each of the amplitude plots increases smoothly as functions of rotor speed from the right side to the left but just after the peak response one observes a rapid falloff of the responses. Numerical integration of the equations of motion indicates that for the responses that are triple valued, the middle amplitude response is unstable and will not be observed. These stability characteristics are illustrated in Fig. 8. The sudden changes in response behavior can be associated with transitions in the neighborhood of these unstable responses.

Conclusions

An analysis that treats the problem of a fully nonlinear helicopter model undergoing ground resonance has been formulated and has been shown to yield accurate predictions of the oscillation amplitudes experienced by a simple rotorcraft model. For small oscillations, the fully nonlinear analysis and

the restricted nonlinear analysis yield essentially identical results. For moderate motions, the fully nonlinear analysis produces a far closer match to numerically obtained results. Both limit-cycle analyses are far more economical to implement than numerical integrations.

The work has laid out a methodology for attacking complex nonlinear interactions and obtaining a compact set of equations for predicting the system's steady-state response. This approach should be fully applicable to a wide variety of nonlinear problems, not just rotorcraft related topics. This research clearly demonstrates how nonlinearities can alter the stability characteristics of a rotorcraft. Inclusion of important nonlinearities in analytical design studies is essential if stability and operational integrity is to be assured.

Acknowledgments

This work was supported by the Army Research Office, Contract 22557-EG. The technical monitor was Gary Anderson.

References

[1]Coleman, R. P., and Feingold, A. M., "Theory of Self Excited Mechanical Oscillations of Helicopter Rotors with Hinged Blades," NACA Rept. 1351, Feb. 1958.

[2]Tongue, B. H., "Limit Cycle Oscillations of a Nonlinear Rotorcraft Model," *AIAA Journal,* Vol. 22, No. 7, 1984, pp. 967-974.

[3]Tongue, B. H., "Response of a Rotorcraft Model with Damping Nonlinearities," *Journal of Sound and Vibration,* Vol. 103, No. 2, 1985, pp. 211-224.

[4]Tang, D. M., and Dowell, E.H., "Effects of Nonlinear Damping in Landing Gear on Helicopter Limit Cycle Responses in Ground Resonance," *Journal of the American Helicopter Society,* Vol. 32, No. 1, 1987, pp. 45-53.

[5]Tang, D. M., and Dowell, E. H., "Influence of Nonlinear Blade Damping on Helicopter Ground Resonance," *Journal of Aircraft,* Vol. 23, No. 2, 1986, pp. 104-110.

[6]Flowers, G. T., "A Study of the Effects of Nonlinearities on the Behavior of Rotorcraft in Ground and Air Resonance," Ph.D. Dissertation, School of Mechanical Engineering, Georgia Inst. of Technology, Dec. 1988.

[7]Tongue, B. H., and Flowers, G.T., "Nonlinear Rotorcraft Analysis," *International Journal of Nonlinear Mechanics,* Vol. 23, No.3, 1988, pp. 189-204.

[8]Bousman, W. G., "A Comparison of Theory and Experiment for Coupled Rotor-Body Stability of a Hingeless Rotor Model in Hover Under Simulated Vacuum Conditions," U.S. Army Aeromechanics Laboratory, NASA Ames Research Center, Moffet Field, CA, 1983.